

On the design of a high-static–low-dynamic stiffness isolator using linear mechanical springs and magnets

A. Carrella^{a,*}, M.J. Brennan^a, T.P. Waters^a, K. Shin^b

^a*Institute of Sound and Vibration Research, University of Southampton, Southampton, Hampshire SO17 1BJ, UK*

^b*School of Mechanical Engineering, Andong National University, 388 Songcheon-Dong, Andong, South Korea*

Accepted 14 January 2008

The peer review of this article was organised by the Guest Editor

Available online 5 March 2008

Abstract

The frequency range over which a linear passive vibration isolator is effective is often limited by the mount stiffness required to support a static load. This can be improved upon by incorporating a negative stiffness element in the mount such that the dynamic stiffness is much less than the static stiffness. In this case, it can be referred to as a high-static–low-dynamic stiffness (HSLDS) mount. This paper is concerned with a theoretical and experimental study of one such mount. It comprises two vertical mechanical springs between which an isolated mass is mounted. At the outer edge of each spring, there is a permanent magnet. In the experimental work reported here, the isolated mass is also a magnet arranged so that it is attracted by the other magnets. Thus, the combination of magnets acts as a negative stiffness counteracting the positive stiffness provided by the mechanical springs. Although the HSLDS suspension system will inevitably be nonlinear, it is shown that for small oscillations the mount considered here is linear. The measured transmissibility is compared with a comparable linear mass–spring–damper system to show the advantages offered by the HSLDS mount.

© 2008 Elsevier Ltd. All rights reserved.

1. Introduction

Improving the performance of vibration isolators continues to be an aim of both engineers and researchers. If an isolator is linear then there is a trade-off between isolation and static deflection [1,2]. To overcome this limitation, it is possible to design the isolator so that its stiffness is nonlinear. A desirable characteristic is a high-static stiffness resulting in a small-static deflection, and a small dynamic stiffness resulting in a low natural frequency and hence a greater frequency range over which there is vibration isolation [3].

There are a number of ways to obtain this desirable nonlinear characteristic. Virgin [4] considered a structure made from a highly deformed elastic element to achieve a softening spring. Platus [5] exploited the buckling of beams under axial load in a specific configuration to achieve a negative stiffness in combination with a positive stiffness, and hence low-dynamic stiffness. Others have achieved the same by connecting linear springs with positive stiffness in parallel with elements of negative stiffness [6–8]. In this paper, a similar

*Corresponding author.

E-mail address: A.Carrella@bristol.ac.uk (A. Carrella).

approach is taken, but the negative stiffness element is achieved by using magnets arranged in an attracting configuration. Magnets have been used in vibration isolation systems in the past, but have often been configured so that they act in repulsion and hence act as springs with positive stiffness. The advantage of such a system is that, for small oscillations, the natural frequency is independent of the isolated mass. Examples of such systems are given in Refs. [9–11]. An interesting example using a pair of magnets in an attracting configuration, which is placed in series with a mechanical spring, has been reported by Mizuno et al. [12]. The series combination of a negative stiffness due to the magnets, with an equal but positive stiffness due to the mechanical spring, results in a system which has infinite stiffness. Although this arrangement is not very useful for vibration isolation, it can be used to obtain very high natural frequencies and significantly reduce the motion of a mass suspended on such a system when subjected to direct rather than base excitation.

A common factor of the approaches using a parallel combination of positive and negative stiffness elements is that it is possible to achieve simultaneously a high-static-low-dynamic stiffness (HSDLS) isolator. These devices are sometimes referred to also as *quasi-zero-stiffness* mechanisms because of their potential capacity of reaching zero dynamic stiffness [3,8].

The aim of this paper is to explore the design of an HSLDS isolator in which positive stiffness from linear springs is counteracted by negative stiffness from attracting magnets. An analytical model of the isolator is derived and the important parameters that govern its effectiveness are determined. A prototype isolator has been built and tested, and its performance is compared with that predicted from the analytical model. To assess the degree of nonlinearity for small oscillations, the nonlinear component of the stiffness force acting on the isolated mass at the static equilibrium position is compared with the linear component of the stiffness force.

2. Theory

The isolator is depicted in Fig. 1. The isolated mass, m , is suspended on two springs each of stiffness k_s , which are connected to a frame that is held together by a stiff round bar. There are three magnets in the

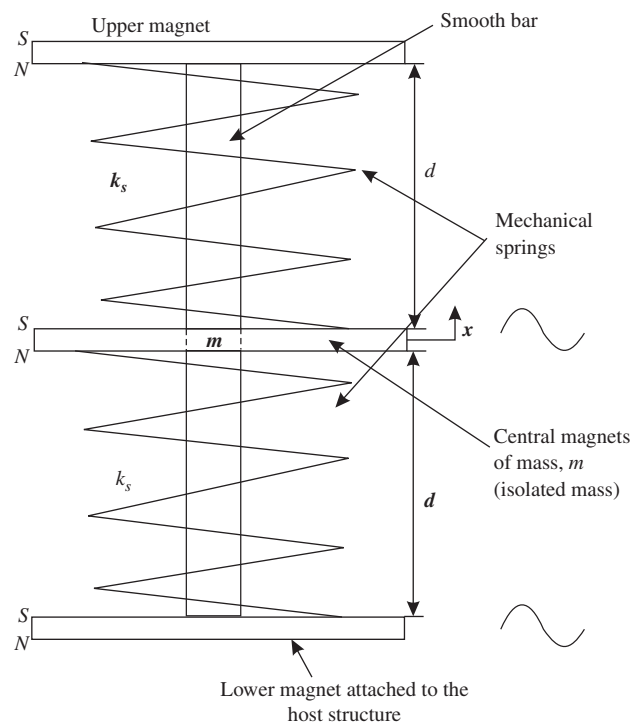


Fig. 1. Schematic of the HSLDS isolator consisting of mechanical springs providing a positive stiffness and the attracting magnets providing a negative stiffness.

isolator arranged in an attracting configuration. The central magnet (which in the experiments reported in Section 3 acts as the isolated mass) has been drilled so that it is free to move in the vertical direction on the smooth round bar, while the other two magnets are fixed with respect to each other. The magnets are thus arranged to act as a negative stiffness opposing that of the mechanical springs.

The magnetic force, f_m , acting between two attracting magnets a distance, d , apart is given by [13]

$$f_m = \frac{C_m}{d^2}, \quad (1)$$

where C_m is the magnetic constant that depends on the strength of the magnets and the medium in which they operate. Considering Eq. (1) and the arrangement of the isolator shown in Fig. 1, the force due to the magnets acting on the mass, m , when it is displaced a distance, x , from the central position is given by

$$f_m = -C_m \frac{4dx}{(d^2 - x^2)^2}. \quad (2)$$

The relationship between an applied force, f , and the displacement of the mass, including the effects of mechanical springs, is thus given by

$$f = 2k_s x - 4C_m \frac{dx}{(d^2 - x^2)^2}. \quad (3)$$

The isolator stiffness can be obtained by differentiating f with respect to x to give

$$k = 2k_s - 4C_m \frac{d(d^2 + 3x^2)}{(d^2 - x^2)^3}. \quad (4)$$

Eqs. (3) and (4) can be written in non-dimensional form, respectively, as

$$\hat{f} = \hat{x} - \alpha \frac{\hat{x}}{(1 - \hat{x}^2)^2} \quad (5)$$

and

$$\hat{k} = 1 - \alpha \frac{(1 + 3\hat{x}^2)}{(1 - \hat{x}^2)^3}, \quad (6)$$

where $\hat{f} = f/2k_s d$, $\hat{x} = x/d$, $\alpha = 2C_m/(k_s d^3)$, $\hat{k} = k/2k_s$ and $-1 \leq \hat{x} \leq 1$. It should be noted that the parameter α is the ratio of the magnitude of stiffness due to the magnets when the mass is in the central position ($\hat{x} = 0$) and the total stiffness of mechanical springs.

Figs. 2(a) and (b) show the non-dimensional force and stiffness as function of the non-dimensional displacement for several values of α . In particular, from Fig. 2(b) it can be seen that the stiffness reaches its maximum $\hat{x} = 0$. The function of the isolator is to achieve a much lower stiffness at the static equilibrium position than is achievable by the mechanical springs alone, i.e. $\hat{k}(0) \ll 1$. Let \hat{k}_0 be the maximum tolerated stiffness. By setting $\hat{x} = 0$ in Eq. (6), the relationship between the parameter α and \hat{k}_0 is given by

$$\hat{k}_0 = 1 - \alpha, \quad (7)$$

which is zero when $\alpha = 1 - \hat{k}_0$. This is to be avoided since, given the softening characteristic of the magnets, the equilibrium position becomes unstable. Rather, a value of \hat{k}_0 is chosen such that $0 < \hat{k}_0 < 1$. There is clearly a trade-off between achieving a low-dynamic stiffness in the vicinity of the equilibrium position and ensuring stability for large excursions from it. Figs. 2(a) and (b) show that the lower the desired stiffness (the higher the value of α) the narrower the displacement range over which there is positive stiffness. The value of the maximum displacement from the equilibrium position before the stiffness becomes zero can be found by setting Eq. (6) to zero and solving for \hat{x} , which yields

$$\hat{x}_{\max} = \sqrt{1 + [\alpha(\sqrt{4 + \alpha} - 2)]^{1/3} - \frac{\alpha}{[\alpha(\sqrt{4 + \alpha} - 2)]^{1/3}}}. \quad (8)$$

To examine the relationship between the maximum displacement \hat{x}_{\max} and the parameter α , it is helpful to simplify Eq. (8) by making some approximations. Using a Taylor-series expansion to third order for small \hat{x} ,

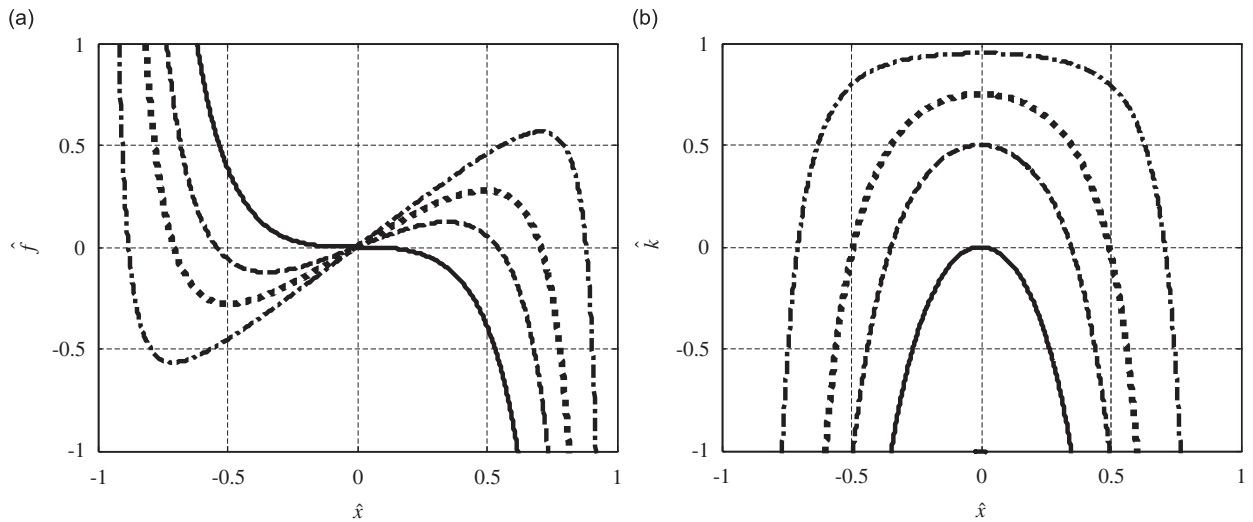


Fig. 2. Static characteristics of the HSLDS isolation mount: (a) force–displacement characteristic and (b) stiffness of the system for different values of the parameter α . Solid line $\alpha = 1$, dashed line $\alpha = 0.5$, dotted line $\alpha = 0.25$ and dash–dotted line $\alpha = 0.05$.

Eq. (5) results in

$$\hat{f} \approx (1 - \alpha)\hat{x} - 2\alpha\hat{x}^3, \tag{9}$$

from which the stiffness can be found by differentiating with respect to \hat{x} , to give

$$\hat{k} \approx (1 - \alpha) - 6\alpha\hat{x}^2. \tag{10}$$

From this approximate expression of the stiffness, the largest displacement from the static equilibrium position before the stiffness becomes zero can be determined. It is given by

$$(\hat{x}_{\max})_{\text{app}} = \sqrt{\frac{1 - \alpha}{6\alpha}}. \tag{11}$$

Both Eqs. (8) and (11) are plotted in Fig. 3. It can be seen that the approximation error is reduced as α increases (in the experimental rig described in the following section $\alpha = 0.72$ and the approximation given by Eq. (11) overestimates the maximum displacement by about 7.5%). From Eq. (7), it can be seen that an increase of α corresponds to a lower maximum stiffness until, in the limit for $\alpha = 1$, it becomes zero. Thus, Fig. 3 illustrates the trade-off between maximum stiffness and available excursion without the stiffness becoming negative.

As mentioned in Section 1, the function of the nonlinear magnetic stiffness is to reduce the overall dynamic stiffness of the isolator. Ideally, this should not cause undesirable nonlinear dynamic behaviour. One way of estimating whether this will occur is to examine the relative contributions of the nonlinear and linear stiffness forces given in Eq. (9). The ratio of these forces is given by $R_{nl} = -2\alpha\hat{x}^2/(1 - \alpha)$, the magnitude of which is plotted in Fig. 4 for $\alpha = 0.72$. It can be seen that the nonlinear component of stiffness is less than about 5% of the linear component of the stiffness provided that the maximum excursion of the mass from the static equilibrium position is less than about $0.1d$. If this condition holds, then the system can be assumed to be approximately linear with constant stiffness given by

$$\hat{k} \approx 1 - \alpha \tag{12}$$

so that the ratio of the natural frequency of the HSLDS isolator ω_n to the natural frequency of the isolator with the mechanical springs alone ω_l , is given by

$$\frac{\omega_n}{\omega_l} = \sqrt{1 - \alpha}. \tag{13}$$

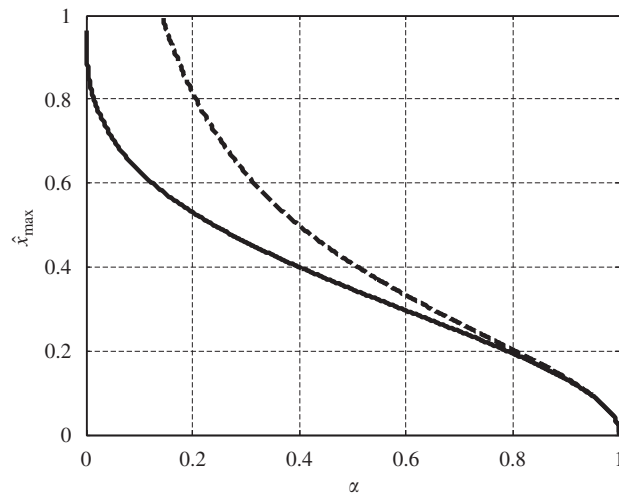


Fig. 3. Maximum non-dimensional displacement from the static equilibrium position for which the mount stiffness is positive as α changes between 0 and its maximum value of 1. The exact expression (solid line) is given by Eq. (8) and the approximate expression (dashed line) is given by Eq. (11).

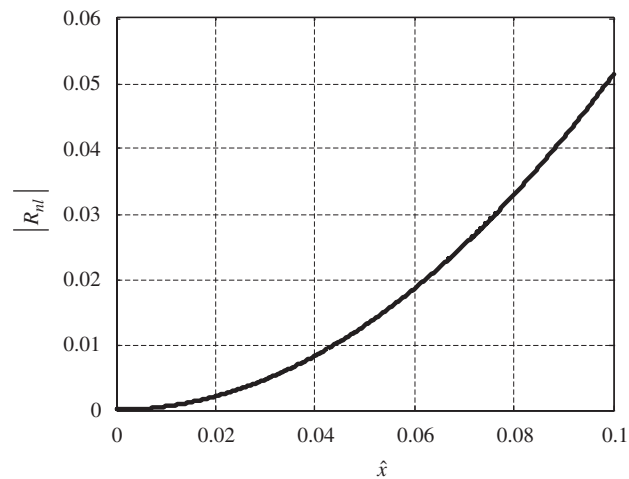


Fig. 4. Ratio between the magnitudes of the nonlinear and linear terms of the restoring force due to the stiffness as a function of the non-dimensional displacement.

Thus, because of the magnets, the frequency at which isolation occurs is reduced by a factor of $\sqrt{1-\alpha}$. There is an additional benefit of lowering the isolator natural frequency if the damping is viscous. The magnitude of the transmissibility of a linear mass–spring–damper system (the system without the magnets) at the resonance frequency ω_l is given approximately $m\omega_l/c$, where m is the isolated mass and c the viscous damping coefficient. Hence, the magnitude of the transmissibility of the HSLDS mount is given by $m\omega_n/c$. It follows that if the viscous damping in the isolator is constant, the peak in the transmissibility is reduced by a factor of $\omega_n/\omega_l = \sqrt{1-\alpha}$.

3. Experiments

A laboratory scale experimental rig was designed and built to illustrate the principle described in Section 2. The HSLDS mount attached to the platform of a vertical shaker is shown in Fig. 5. Similar to the model described above, it comprises three magnets, two coil springs and a smooth central round bar. Two magnets

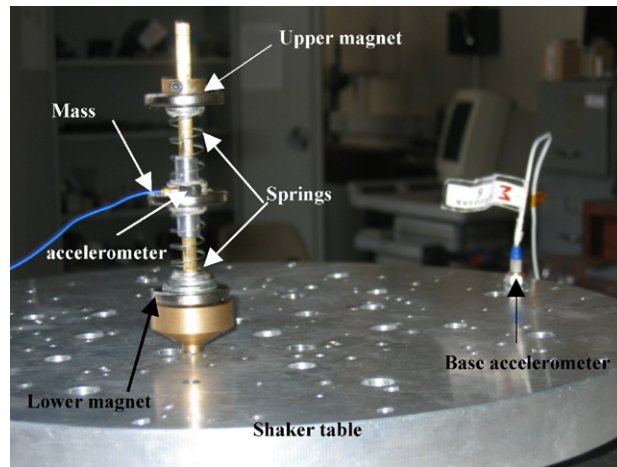


Fig. 5. Experimental rig showing the HSLDS mount attached to the shaker table.

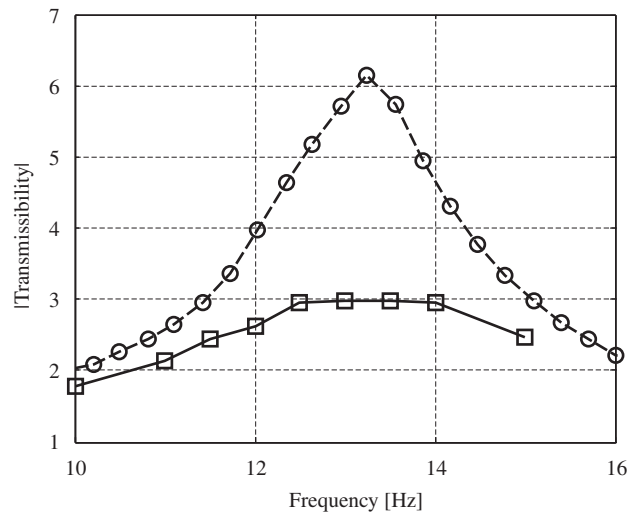


Fig. 6. Measured transmissibility to determine the mount properties. Transmissibility of the system without the coil springs and the magnets arranged in a repelling configuration (dashed line). Transmissibility of the mass–spring system without the magnets at the extremities of the bar (solid line).

were fixed at the top and the bottom of the bar at a distance $d = 3.81$ cm from the central magnet of mass 0.04 kg, which was free to move vertically, sliding on the central bar. To take into account the static displacement of the isolated mass due to gravity and ensure symmetry of the magnetic force, a washer of about 2 mm was inserted between the lower spring and the magnet to which it was attached.

The main aim of the experiment was to compare the transmissibility curves of the isolator with that of a conventional mass–spring system, which was realised by simply replacing the magnets at each end of the central bar with non-magnetic elements.

First, the magnetic constant, C_m , was measured. For this purpose, the springs were removed and the central magnet was reversed, so that it was repelled by those at the extremities of the shaft. The mean distance between the magnets at each end of the central bar and the central magnet was 3.4 cm. In this case, the stiffness had a hardening characteristic. However, the isolator was excited using a stepped-sine generated by an HP analyser 35656A such that the relative amplitude between the base and the suspended mass was small. Thus, it was possible to assume that the stiffness was constant. The dashed line in Fig. 6 shows the absolute value of the ratio between the acceleration of the suspended mass and the acceleration of the base (transmissibility).

The peak occurs at the resonance frequency at about 13.25 Hz which, given the oscillating mass, gives the stiffness to be 277.23 N/m. Setting $x = 0$, $k_s = 0$ and $k = 277.23$ N/m in Eq. (4) results in

$$C_m = 2.72 \times 10^{-3} \text{ N m}^2. \quad (14)$$

Second, the stiffness of the springs was measured by suspending the mass only on the two springs and removing the lower and upper magnets (equivalent linear system). The corresponding transmissibility measurement is shown as a solid line in Fig. 6. It can be seen that the resonance peak is at a frequency of 13.1 Hz, which means that the combined stiffness of the springs is

$$2k_s = 271 \text{ N/m}. \quad (15)$$

The non-dimensional parameter α can thus be calculated:

$$\alpha = \frac{C_m}{k_s d^3} \approx 0.72. \quad (16)$$

From Eq. (13), the natural frequency of the HSLDS system is, therefore, predicted to be about 7 Hz.

Having estimated the natural frequency of the HSLDS isolator, an experiment was conducted to see if the isolator performed as expected. It was assembled as shown in Fig. 5 and placed on the vertical shaker. It was excited at discrete frequencies from 6 to 10 Hz, and the base displacement amplitude of 3 mm was kept constant throughout the tests. Acceleration of the base and the isolated mass was measured using one PCB type 352C22 and one ENDEVCO 2256-100 model accelerometers. At each frequency, once the system was at steady state, 15 s of data were captured using an NI DAQPad-6020E acquisition card. The ratio of the rms acceleration of the isolated mass to the rms acceleration of the base was calculated for each excitation frequency and this is plotted in Fig. 7, where it is labelled as transmissibility. This was repeated for an excitation level of 4 mm and this is also plotted in Fig. 7. As well as these graphs, the transmissibility of the isolator without the magnets fitted is also plotted for comparison. It can be seen that the HSLDS stiffness system has a peak at 7 Hz as predicted, which is roughly half that of the isolator without the magnets. It should be noted that the amplitude of vibration at the resonance frequency has also been reduced by a factor of two, which is in line with that expected for a system with viscous damping.

To assess whether the HSLDS isolator was behaving as a linear system, the spectral content of the acceleration time history of the isolated mass was calculated for each excitation frequency. As expected from a system with cubic nonlinearity, odd higher order harmonics were observed. In Fig. 8, the ratio between the largest perceptible higher order harmonic (the third), $|A_3|$, and that at the excitation frequency, $|A_1|$, are plotted. It can be seen that the amplitude of the third harmonic is about 30 times less than that of the

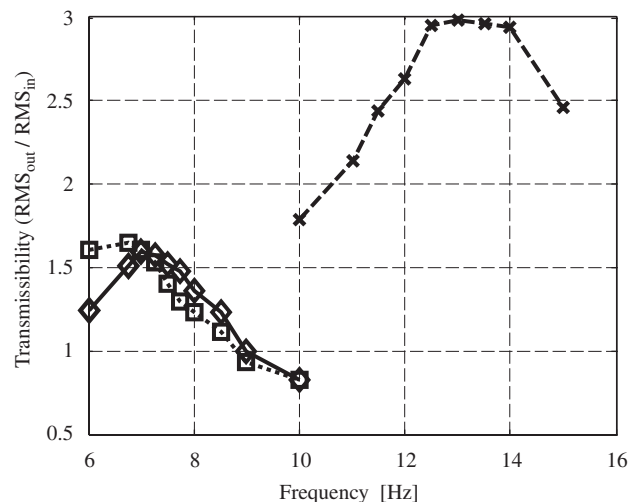


Fig. 7. Comparison of the transmissibility of a linear mass–spring system (dashed line and crosses) and that of the HSLDS mount for a 3 mm base amplitude excitation (solid line and diamonds) and 4 mm base amplitude excitation (dotted line and squares).

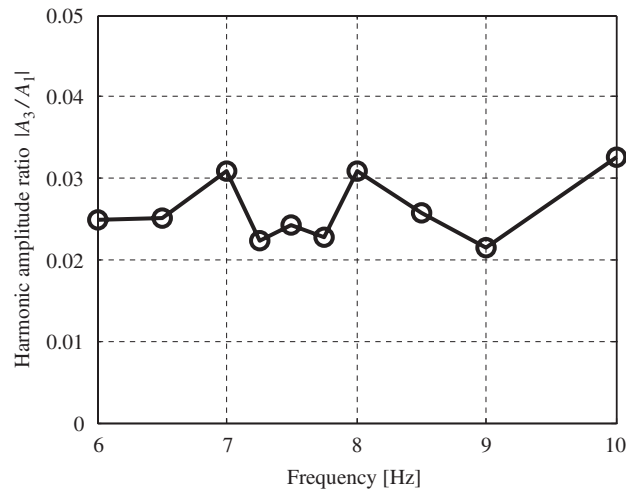


Fig. 8. Ratio between the third and first harmonics of the measured response of the HSLDS system at each excitation frequency.

fundamental frequency $|A_1|$ for each frequency of excitation. This demonstrates that the nonlinearity in the isolator is very weak for the excitation levels used.

4. Discussion

In the static analysis of the HSLDS isolator, the magnetic force was modelled using Coulomb's law. Despite this being a very simple model, the analytical predictions and the experimental results agree reasonably well. It can be seen from Fig. 7 that the peak transmissibility was about 1.5, which means that the absolute motion of the isolated mass was about 6 mm for a 4 mm base displacement, and hence the relative displacement between the isolated mass and the base was about 2 mm. This is about 5.25% of the distance between the central magnet and the end magnets, which means that the nonlinear component of the force is about 1.5% of the linear component; so the nonlinearity is negligible for this isolator when subjected to reasonably high base excitation levels (4 mm). The main advantage of the HSLDS system is its load-bearing capability. Reducing the natural frequency by a factor of two would be possible by using springs four times softer. A suspended mass of 40 g will have a natural frequency of 7 Hz if it is suspended on a spring with a coefficient of 77.5 N/m. However, this would mean a static displacement of 5 mm. With the HSLDS mount the static displacement is dependent only on the coil springs, which have a combined stiffness of 271 N/m resulting in a static displacement of only 1.5 mm.

5. Conclusions

The static and linearised dynamic behaviour of an HSLDS isolator has been investigated. The isolator consisted of mechanical springs providing a positive stiffness and magnets in an attracting configuration providing a negative stiffness. The combination of the mechanical stiffness and the nonlinear stiffness of the magnets results in a device that has HSLDS characteristics. A test rig was built using off-the-shelf magnets and coil springs to demonstrate the practicality of the proposed device and to validate the mathematical model. A reduction in the natural frequency by a factor of two from about 14 to 7 Hz was achieved by using the magnets, and the measured transmissibility from a displacement input showed that the device behaved approximately linearly.

Acknowledgement

The authors would like to thank Mr. Luigi Scala of Mollificio Guidi s.r.l. (Italy) for technical assistance and the supply of coil springs.

References

- [1] J. Den Hartog, *Mechanical Vibrations*, McGraw-Hill, New York, 1956.
- [2] Harris, *Shock and Vibrations Handbook*, fifth ed., McGraw-Hill, New York, 2002.
- [3] E.I. Rivin, *Passive Vibration Isolation*, ASME, New York, 2001.
- [4] L.N. Virgin, S.T. Santillan, R.H. Plaut, Vibration isolation using extreme geometric nonlinearity, *Euromech Colloquium 483 Geometrically Non-linear Vibrations of Structures*, Porto, Portugal, 9–11 July 2007.
- [5] D.L. Platus, Negative-stiffness-mechanism vibration isolation systems, *Proceedings of SPIE, Vibration Control in Microelectronics, Optics, and Metrology* 161 (1992) 44–54.
- [6] S.E. Woodard, J.M. Housner, Nonlinear behavior of a passive zerospring-rate suspension system, *Journal of Guidance, Control, and Dynamics* 14 (1991) 84–89.
- [7] P. Alabuzhev, A. Gritchin, L. Kim, G. Migirenko, V. Chon, P. Stepanov, *Vibration Protecting and Measuring Systems with Quasi-Zero Stiffness*, Hemisphere, New York, 1989.
- [8] A. Carrella, M.J. Brennan, T.P. Waters, Static analysis of a quasi-zero-stiffness vibration isolator, *Journal of Sound and Vibration* 301 (3–5) (2007) 678–689.
- [9] E. Puppini, V. Fratello, Vibration isolation with magnet springs, *Review of Scientific Instruments* 73 (11) (2002) 4034–4036.
- [10] A. D'Angola, G. Carbone, L. Mangialardi, C. Serio, Nonlinear oscillations in a passive magnetic suspension, *International Journal of Nonlinear Mechanics* 41 (2006) 1039–1049.
- [11] E. Bonisoli, A. Vigliani, Identification techniques applied to a passive elasto-magnetic suspension, *Mechanical Systems and Signal Processing* 21 (2007) 1479–1488.
- [12] T. Mizuno, M. Takasaki, D. Kishita, K. Hirakawa, Vibration isolation system combining zero-power magnetic suspension with springs, *Control Engineering Practice* 15 (2007) 187–196.
- [13] M. McCaig, *Permanent Magnets in Theory and Practice*, Pentech Press, Plymouth, 1977.